International Journal of Nanomedicine

Dovepress

open access to scientific and medical research

Open Access Full Text Article

ORIGINAL RESEARCH

Antibacterial and Antifungal Efficacy of Medium and Low Weight Chitosan-Shelled Nanodroplets for the Treatment of Infected Chronic Wounds

Narcisa Mandras[1], Monica Argenziano[2], Mauro Prato[1], Janira Roana[1], Anna Luganini[3], Valeria Allizond[1], Vivian Tullio[1], Nicole Finesso[4], Sara Comini[1], Bruno Emilio Bressan[4], Francesca Pecoraro[4], Giuliana Giribaldi[4], Adriano Troia[5], Roberta Cavalli[2], Anna Maria Cuffini[1,*], Giuliana Banche[1,*]

[1]Department of Public Health and Pediatric Sciences, University of Torino, Turin, 10126, Italy; [2]Department of Drug Science and Technology, University of Torino, Turin, 10125, Italy; [3]Department of Life Sciences and Systems Biology, University of Torino, Turin, 10123, Italy; [4]Department of Oncology, University of Torino, Turin, 10126, Italy; [5]Istituto Nazionale di Ricerca Metrologica, Turin, 10135, Italy

*These authors contributed equally to this work

Correspondence: Valeria Allizond, Department of Public Health and Pediatric Sciences, University of Torino, Via Santena 9, Turin, 10126, Italy, Tel +390116705644, Fax +390112365644, Email valeria.allizond@unito.it

Purpose: Medium versus low weight (MW vs LW) chitosan-shelled oxygen-loaded nanodroplets (cOLNDs) and oxygen-free nanodroplets (cOFNDs) were comparatively challenged for biocompatibility on human keratinocytes, for antimicrobial activity against four common infectious agents of chronic wounds (CWs) – methicillin-resistant *Staphylococcus aureus* (MRSA), *Streptococcus pyogenes, Candida albicans* and *C. glabrata* – and for their physical interaction with cell walls/membranes.

Methods: cNDs were characterized for morphology and physico-chemical properties by microscopy and dynamic light scattering. In vitro oxygen release from cOLNDs was measured through an oximeter. ND biocompatibility and ability to promote wound healing in human normoxic/hypoxic skin cells were challenged by LDH and MTT assays using keratinocytes. ND antimicrobial activity was investigated by monitoring upon incubation with/without MW or LW cOLNDs/cOFNDs either bacteria or yeast growth over time. The mechanical interaction between NDs and microorganisms was also assessed by confocal microscopy.

Results: LW cNDs appeared less toxic to keratinocytes than MW cNDs. Based on cell counts, either MW or LW cOLNDs and cOFNDs displayed long-term antimicrobial efficacy against *S. pyogenes, C. albicans*, and *C. glabrata* (up to 24 h), whereas a short-term cytostatic effects against MRSA (up to 6 h) was revealed. The internalization of all ND formulations by all four microorganisms, already after 3 h of incubation, was showed, with the only exception to MW cOLNDs/cOFNDs that adhered to MRSA walls without being internalized even after 24 h.

Conclusion: cNDs exerted bacteriostatic and fungistatic effects, due to the presence of chitosan in the outer shell and independently of oxygen addition in the inner core. The duration of such effects strictly depends on the characteristics of each microbial species, and not on the molecular weight of chitosan in ND shells. However, LW chitosan was better tolerated by human keratinocytes than MW. For these reasons, the use of LW NDs should be recommended in future research to assess cOLND efficacy for the treatment of infected CWs.

Keywords: chitosan nanodroplets, methicillin-resistant *Staphylococcus aureus*, *Streptococcus pyogenes*, *Candida* spp, chronic wounds

Introduction

Chronic wounds (CWs) – nonhealing breaks of the skin epithelial continuity longer than 42 days – are usually characterised by persistent hypoxia, intensified inflammation, and altered balances between matrix metallo-proteinases (MMPs) and their endogenous inhibitors; moreover, microbial infection frequently complicates CW status.[1–4] CWs affect

Received: 14 December 2021
Accepted: 15 March 2022
Published: 14 April 2022

a large fraction of the population worldwide – especially the elderly – jeopardising the physical health and the economic system of industrialised countries. It is estimated that 1% to 2% of the population will experience a CW during their lifetime.[5] For this reason, it is important to find more effective treatments to heal CWs and to prevent serious complications such as infections, which can lead to amputation, to improve health of patients.[6]

One of the most important problems to solve, in managing CWs, is the lack of oxygen due to persistent tissue hypoxia. Oxygen is essential during the healing process, as a consequence, an inappropriate delivery of O_2-rich blood to the wound tissue obstacles the physiological healing course.[7] Another important issue to deal with is medical therapy; in fact, topical oxygen therapy, despite being cheap and associated with low toxicity, is not always able to trespass the skin *stratum corneum* and to deliver the proper oxygen amount to fibroblasts, keratinocytes, and inflammatory cells to fully restore their functions.[8–10]

The current situation is also worsened by antimicrobial wound management, representing an urgent challenge and requiring new solutions with respect to antimicrobials applied topically for a long time, attempting to prevent infections by human pathogens. Therefore, any treatments able to heal a significant percentage of wounds quickly, completely and persistently, would substantially not only improve the clinical outcomes but also reduce the overall costs.[6] Depending on the etiopathological agent, skin infections differ in severity, from simple pustular lesions of the integument to more spreading diseases.[11] In particular, as emerged from bacterial profiling of CWs, the most commonly isolated bacterial species (spp) are as follows: *Staphylococcus aureus* (93.5%), *Enterococcus faecalis* (71.1%), *Pseudomonas aeruginosa* (52.2%), coagulase-negative *Staphylococcus* spp (45.7%), *Proteus* spp (43.1%) and anaerobic bacteria (39.1%).[12] In this context, it should be noticed that microbial wound colonization (mainly due to *S. aureus, P. aeruginosa* and *S. pyogenes*) was proved responsible for a further delay in wound recovery, and it is additionally hampered by the development of drug resistance.[13–15]

Along with bacteria, fungal infections are often involved in worsening and delaying the healing process of CWs too, being a common cause of morbidity, mortality and cost in critical care population.[16–18] Ballard et al reported that fungi were isolated at least once from 6.3% of burn patients, with positive cultures obtained from the wound itself.[17] *C. albicans* is the main yeast isolated in fungal infections nevertheless, non-*albicans Candida* species now represent a substantial portion of isolates identified in hospitals worldwide, with a noticeable clinical relevance to *C. glabrata, C. tropicalis, C. parapsilosis*, and *C. krusei*.[19–21]

Chitosan is one of the natural polymers which raised a strong interest for researchers due to some exceptional properties such as biocompatibility, non-toxicity, low-cost and other pharmacological properties, such as antimicrobial, antitumor, antioxidant, antidiabetic, immunoenhancing.[22,23] The latest advances in chitosan-based antimicrobial materials revealed a potent anti-bacterial and anti-fungal capacity.[22–24] These data are in line with those of Rocha Neto et al[25] who reported that a bi-layer film of chitosan and hyaluronic acid allowed a potent anti-*E. coli* effect. Some researches highlighted also that artificial hydrogels modified with chitosan exerted antibacterial efficacy against both *S. aureus* and *E. coli*.[26,27] Additionally, in the work of Feng et al,[28] the hybrid coating of titanium with chitosan and MoS_2 exhibited a high antibacterial efficacy, *versus E. coli* and *S. aureus*, respect to pure titanium, and the effect was further enhanced by using both photodynamic and photothermal irradiation. Of note, the antimicrobial activity of chitosan depends on several factors related to chitosan (molecular weight, deacetylation degree, concentration), microorganism (species, cell age) and environmental factors (pH, presence of metal cations, temperature).[22,23]

In this scenario, nanotechnologies had played an important role, and the development of new nanocarriers filled with oxygen-solving fluorocarbons and shelled with polysaccharides – displaying antimicrobial properties – has paved the way for new nanotherapies, mainly nanodroplets (NDs), in CW management able to counteract hypoxia in pathological tissues.[29–32] Structurally, these nanocarriers are characterised by typical outer polysaccharide-based shells and inner fluorocarbon cores. In a previous work of our research group, it emerged that medium weight (MW) chitosan is the best candidate polysaccharide, for the outer shell of NDs, due to its anti-inflammatory and antimicrobial properties.[33] However, for the inner core, the 2H,3H-decafluoropentane (DFP) has the advantage to bind oxygen not only through van der Waals forces but also through hydrogen intermolecular bonds.[34] Consequently, DFP, in oxygen-loaded (OL) NDs, binds oxygen molecules more efficiently, allowing slow and gradual oxygen release over time. Additionally, NDs keep peculiar characteristics including size, surface charge, stability, biocompatibility, and responsiveness to ultrasound (US), which contribute to deliver oxygen or drugs through cell membranes.[31,32,35]

Based on these promising qualities, chitosan-shelled oxygen loaded nanodroplets (cOLNDs) have been presented as innovative, nonconventional, cost-effective, and nontoxic therapeutic tools to be potentially employed to restore the physiological invasive phenotype of immune cells in hypoxia-associated inflammation, but also preeclampsia and cancer.[36–38]

In a previous research, we demonstrated that, even if MW chitosan had good performance as a shell component in cOLNDs, it revealed mild biocompatibility with human keratinocytes, whereas low weight (LW) chitosan in cOLNDs was associated with better physico-chemical characteristics and higher biocompatibility with skin cells.[39] Additionally, LW cOLNDs were proved effective in restoring normoxia-like migratory phenotypes of human keratinocytes in hypoxic conditions, thereby promoting the activation of wound healing processes. However, no data on the effects of LW cOLNDs on fungi and bacteria are still available.

For these reasons, in the present work, after preliminary checking of standard physico-chemical characteristics and biocompatibility with human keratinocytes, MW and LW cOLNDs, as well as oxygen-free nanodroplets (cOFNDs), were comparatively challenged for their antimicrobial activity against four common infectious agents of CWs: methicillin-resistant *S. aureus* (MRSA), *S. pyogenes, C. albicans* and *C. glabrata*. Complementary analysis by confocal microscopy was also performed to study the physical interaction between NDs and cell walls/membranes.

Materials and Methods

Manufacturing of Oxygen-Loaded Nanodroplets and Control Formulations

OLND formulations were produced according to the preparation protocol previously described in detail.[39] Briefly, an ethanol solution (Carlo Erba, Cornaredo, Italy) containing 1% w/v of Epikuron® 200 (Degussa, Hamburg, Germany) and palmitic acid was mixed with DFP (Fluka, Buchs, Switzerland) under magnetic stirring to produce a pre-emulsion. A phosphate buffered saline (PBS) solution was then added, and the sample was homogenized for 2 min using an Ultra-Turrax SG215 homogenizer (IKA, Staufen, Germany). Thereafter, oxygen was supplied to the obtained nanosuspension for 2 min. Finally, a drop-wise addition of an aqueous solution of MW chitosan (degree of deacetylation 75–85%, 190–310 KDa, Sigma-Aldrich, Saint Louis, USA) or LW chitosan (degree of deacetylation 75–85%, 50–190 KDa, Sigma-Aldrich) (2.7% w/v, pH 4.5) was performed under magnetic stirring to obtain the chitosan-shelled NDs. To produce OFNDs the addition of oxygen was skipped. Similarly, oxygen-saturated solution (OSS) was obtained by saturating a PBS solution with oxygen. For selected experiments (confocal microscopy studies), fluorescent labelled ND formulations were prepared via conjugation of chitosan with fluorescein isothiocyanate (FITC, Sigma-Aldrich; FITC concentration: 10% for studies on human cells and 7% for studies on microbial cells).

Nanodroplet in vitro Characterization

The NDs were in vitro characterized from the physico-chemical point of view, as previously described.[31,39] The morphology of NDs was assessed by transmission electron microscopy (TEM) using a Philips CM10 instrument (Eindhoven, The Netherlands). The samples were dropped onto a Formvar-coated copper grid and air-dried before observation.

Dynamic light scattering was used to determine the average diameters, polydispersity indexes, and zeta potentials of NDs, as previously detailed.[31,39] The tests were carried out on ND samples diluted in deionized water at a scattering angle of 90° and at a temperature of 25°C using a 90Plus Particle Size Analyzer (Brookhaven, New York City, NY, USA). To determine the zeta potential, ND samples were placed in an electrophoretic cell, where an electric field of 15 V/cm was applied. Using the Smoluchowski equation, the electrophoretic mobility was translated to a zeta potential value.[40] Each analysis was performed in triplicate. The osmolarity and viscosity of the NDs were measured at 25°C using a Knauer osmometer and an Ubbelohde capillary viscosimeter (Schott Gerate, Mainz, Germany), respectively.

The oxygen content of OLNDs was determined by quantifying with a gravimetric method the produced sodium sulphate after the addition of known amounts of sodium sulphite to the samples.[39] Moreover, the oxygen release kinetics from OLNDs were in vitro evaluated by a dialysis method. A dialysis bag (Spectra/Por cellulose dialysis membrane, cut-off 12,000–14,000 Da) containing the MW or LW OLNDs was placed in a hypoxic receiving medium (NaCl 0.9% w/v

solution having an oxygen concentration decreased by an N_2 purge to 1 mg/L). The oxygen concentration released from the OLND samples into the hypoxic receiving phase was measured using Hach Lange LDO oximeter, at fixed times up to 24 h. The oxygen released by an oxygen-saturated solution was also evaluated as control. The oximeter was calibrated in air before each analysis until stable temperature, and humidity conditions were achieved.

All ND formulations were sterilized through UV-C exposure for 20 min, as previously described in detail.[39]

Nanodroplet Biocompatibility Assessment by Cytotoxicity and Cell Viability Tests

Human Cells

HaCaT cell line, immortalized from a 62-year-old Caucasian male donor, was used as a source of human keratinocytes, and it was obtained from the American Type Culture Collection (Manassas, VA, USA). HaCaT cells were grown in a humidified CO_2/air-incubator at 37°C as monolayers in Dulbecco's Modified Eagle Medium – high glucose (DMEM HG) supplemented with 10% foetal bovine serum, 100 U/mL penicillin, 100 µg/mL streptomycin and 2 mM L-glutamine.

Determination of Nanodroplets Cytotoxicity on Human Cells by Lactate Dehydrogenase Assay

The possible cytotoxic action of NDs was evaluated as the release of lactate dehydrogenase (LDH) by the cells in the extracellular environment.

Cells were cultured in 6-well plates (3×10^5 cells/well) in 2 mL/well of integrated cell culture medium, at regular conditions with 5% CO_2 at 37°C overnight to allow cell adhesion. Then, the cells were treated or not with 10% v/v MW or LW cOLNDs and cOFNDs and exposed to normoxia (20% O_2) in a normal CO_2 cell culture incubator or hypoxia (1% O_2) in a hypoxia chamber, for different times. Sterile water was placed inside the chamber to maintain moist conditions. Hypoxic condition was created by filling the chamber with 1% O_2, 5% CO_2 and balanced N_2. The chamber was sealed and placed in a 37°C cell culture incubator.

Following exposure-times, the medium was harvested and centrifuged at 13,000 g for 30 min at room temperature, while the cells, after being scrapped and washed with PBS, were resuspended in triethanolamine solution (TRAP) and sonicated. Five µL of cell lysates and 50 µL of cell supernatants were diluted with TRAP and more with 0.5 mM sodium pyruvate and 0.25 mM reduced form of nicotinamide adenine dinucleotide (NADH). Results were analyzed by measuring the absorbance at 340 nm (Synergy HT microplate reader), and cytotoxicity was presented as the ratio of extracellular to total (intracellular+ extracellular) LDH activity. LDH activities (intracellular and extracellular) were expressed as µmol of oxidized NADH/min/well.

Evaluation of Nanodroplet Action on Cell Viability by 3-(4,5-dimethylthiazol-2-yl)-2,5-Diphenyltetrazolium Bromide Assay

The MTT (3-[4,5-dimethylthiazol-2-yl]-2,5-diphenyltetrazolium bromide) assay was used to evaluate cell viability and was based on the protocol described by Argenziano et al.[39] Cells were incubated for 24 h without or with 10% v/v MW or LW cOLNDs and cOFNDs, and exposed to normoxia (20% O_2) in a normal CO_2 cell culture incubator or hypoxia (1% O_2) in a hypoxia chamber at 37°C, as above detailed. Results were analyzed with the Synergy HT reader at a test wavelength of 550 nm and at a reference wavelength of 650 nm. The data were expressed as viability percentages.

Bacteria and Yeasts

Clinical microbial strains were isolated from human ulcerated wounds of patients from Infermi Hospital (Biella, Italy). These strains are part of the collection of the Bacteriology and Mycology Laboratory, thus no institutional review board or ethics committee is necessary. MRSA were cultured on Mannitol Salt Agar (MSA; Oxoid SpA, Rodano, Italy), *S. pyogenes* on Trypticase Soy Agar (TSA; Oxoid SpA), and *Candida* spp. on Sabouraud dextrose (SAB agar; Oxoid SpA) at 37°C.

Evaluation of Nanodroplet Uptake by Bacteria and Yeasts Through Confocal Microscopy Analyses

MRSA and *S. pyogenes* [10^9 colony forming units (CFUs)/mL] were incubated without or with 10% v/v FITC-labeled OLNDs or OFNDs for 3 h and 24 h with agitation at 37°C. At each incubation time, bacteria and different formulation suspensions (50 µL) were transferred on glass slides, dried in air, and subsequently stained with 5 µg/mL PI in a humid chamber at 37°C for 15 min.

C. albicans and *C. glabrata* (10^8 CFUs/mL) were stained with 10 µg/mL PI and incubated without or with 10% v/v FITC-labeled OLNDs or OFNDs, for 3 h and 24 h with agitation at 37°C. Then, 10 µg/mL propidium iodide (PI) was added to the mix for 1 h at 37°C and at each incubation time, 100 µL suspensions from yeasts and different formulations were transferred on glass slides.

For microscopy analysis, bacteria and yeasts were mounted in a mounting medium and covered by cover slips. Samples were examined using an Olympus IX70 inverted laser scanning confocal microscope, and images were captured using FluoView 300 software (Olympus Biosystems).

In vitro Determination of Anti-Bacterial and Anti-Fungal Activity of Nanodroplets

MRSA and *S. pyogenes* (10^4 CFUs/mL) or *C. albicans* and *C. glabrata* (10^5 CFUs/mL) were, respectively, incubated in Trypticase Soy Broth (TSB; Oxoid SpA) alone (control) or in SAB broth alone (control) or with 10% v/v OSS, 0.139% MW or LW chitosan solution, and MW or LW cOFND or cOLND formulations for 4, 6, and 24 h at 37°C. At the different incubation time, serial dilutions from each sample, in 0.9% NaCl saline solution, were obtained, spread on suitable agar, and then incubated at 37°C for 24 h, to achieve the number of CFU/mL.

Statistical Analysis

For every investigational study, at least three independent experiments were executed, and each condition was performed at least in duplicate. Data were expressed as means ± standard errors of the mean (SEM), whereas representative pictures for imaging results were selected. All data were analyzed for significance by a one-way analysis of variance (ANOVA) followed by Tukey's post hoc test (GraphPad Software San Diego, USA). A p value <0.05 was deemed significant.

Results

The physico-chemical characteristics of ND formulations either loaded with oxygen or unloaded are reported in Table 1.

The sizes of NDs were in the nanometer range (~300–550 nm as average diameters), with LW cOLND diameters (~400 nm) being smaller than MW cOLND diameters (~550 nm), and all OLNDs being larger than their oxygen-free counterpart. These results were supported by TEM analysis, which revealed the ND spherical shape and core-shell structure (data not shown). All polydispersity indexes were included between 0.19 (MW cOLNDs) and 0.22 (LW cOLNDs). Zeta potentials ranged from +30.20 mV (MW cOLNDs) to +32.46 mV (LW cOLNDs). Either MW or LW cOLNDs showed a similar oxygen content (~35 mg/L). The OLND capability to release oxygen in a hypoxic receiving

Table 1 Physico-Chemical Characterization of ND Formulations

Formulation	Average Diameter ± SD (nm)	Polydispersity Index ± SD	Zeta Potential ± SD (mV)	Osmolarity ± SD (mOsm)	Viscosity ± SD (cP)
LW cOFNDs	305.3 ± 18.5	0.20 ± 0.02	31.95 ± 3.05	285 ± 0.4	1.34 ± 0.02
MW cOFNDs	360.8 ± 25.3	0.21 ± 0.01	30.45 ± 2.46	284 ± 0.3	1.39 ± 0.02
LW cOLNDs	420.4 ± 20.7	0.22 ± 0.02	32.46 ± 2.98	282 ± 0.6	1.32 ± 0.01
MW cOLNDs	545.7 ± 32.1	0.19 ± 0.01	30.20 ± 2.86	284 ± 0.5	1.38 ± 0.02

Notes: MW or LW cNDs either loaded with oxygen (cOLNDs) or unloaded (cOFNDs) were in vitro characterized measuring their average diameter, polydispersity index and zeta potential by dynamic light scattering. Osmolarity and viscosity were determined using an osmometer and an Ubbelohde capillary viscosimeter, respectively. Results are shown as mean ± SD from ten ND formulations.

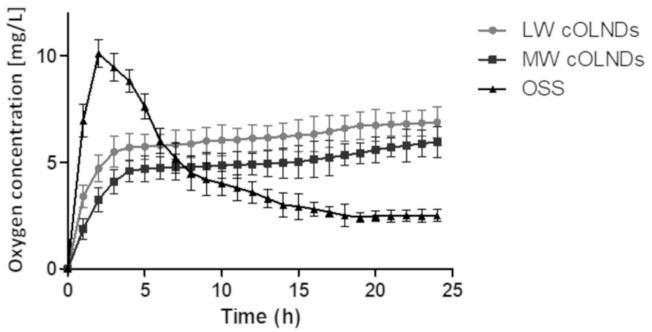

Figure 1 In vitro oxygen release kinetics from cOLNDs and oxygen-saturated solution (OSS). The LW or MW cOLND capability to release oxygen in a hypoxic receiving phase was evaluated through an oximeter. Results are shown as mean ± SD from three independent experiments.

phase was in vitro investigated in comparison with an OSS (Figure 1). The oxygen was released from both the cOLNDs by passive diffusion with a prolonged release kinetics of up to 24 h. No significant differences in the release profile were observed between the two types of OLNDs. On the contrary, oxygen from the OSS diffused quickly in the hypoxic phase but then the oxygen concentration decreased rapidly.

As showed in (Figure 2A), MW cOFNDs significantly ($p<0.001$) reduced viability of human keratinocytes, either in normoxic or hypoxic conditions, determining an increase in cytotoxicity percentages with respect to controls. On the contrary, no cytotoxic effect was exerted by both MW cOLNDs and LW cOFNDs/cOLNDs (Figure 2A). These data were further confirmed by the MTT results (Figure 2B): a significant ($p<0.001$ and $p<0.05$) decrease into HaCaT cells viability percentages, compared to controls, in the presence of MW cOFNDs, in both oxygen conditions, was obtained. Additionally, only in hypoxia, also MW cOLNDs and LW cOFNDs/cOLNDs determined a significant ($p<0.05$) reduction into viability percentages of human keratinocytes (Figure 2B).

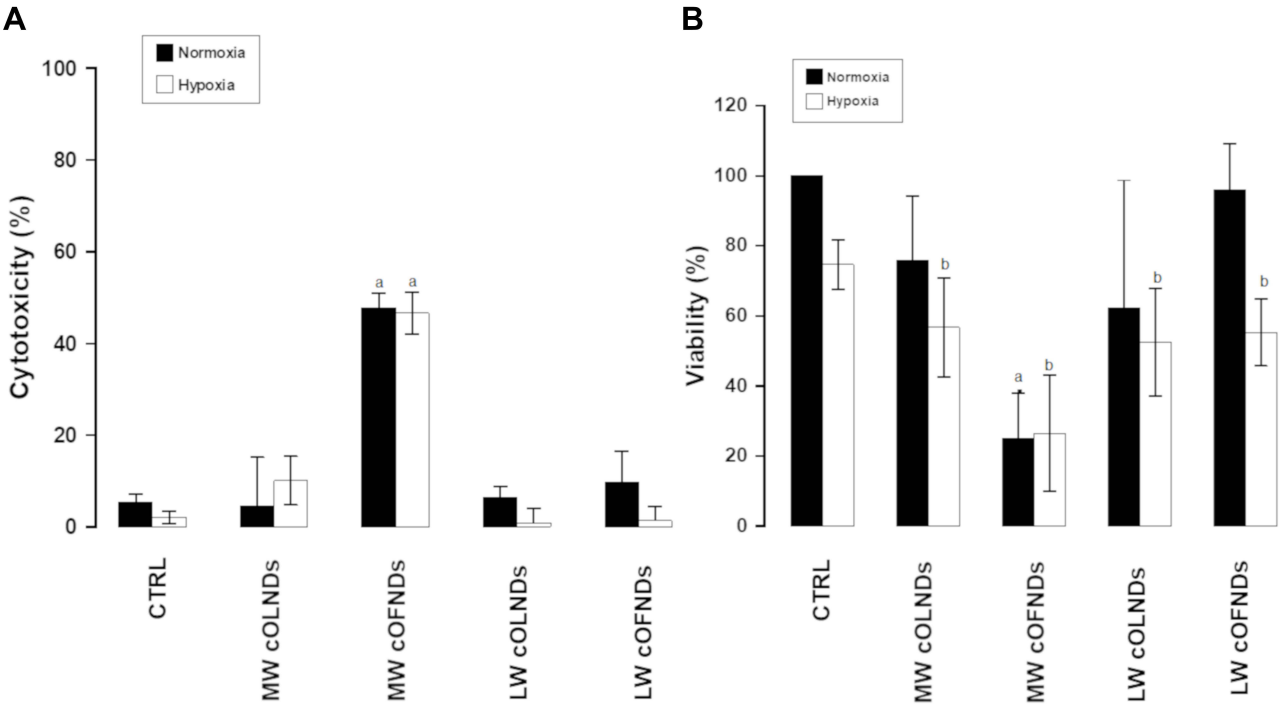

Figure 2 cND cytotoxicity and effects on human keratinocyte viability, under normoxic and hypoxic conditions. HaCaT cells (3x 10^5 cells/mL for LDH studies and 1.6×10^5 cells/mL for MTT studies) were left untreated or treated with MW or LW cOLNDs and cOFNDs for 24 h in normoxia (20% O_2, black columns) or hypoxia (1% O_2, white columns). After collection of cell supernatants and lysates, cytotoxicity percentage was measured through LDH assay (**A**) and cell viability percentage was measured through MTT assay (**B**). Results are shown as means ± SEM from three independent experiments. Data were also evaluated for significance by ANOVA. Vs normoxic control cells: [a] $p<0.001$; vs hypoxic control cells: [b] $p<0.05$.

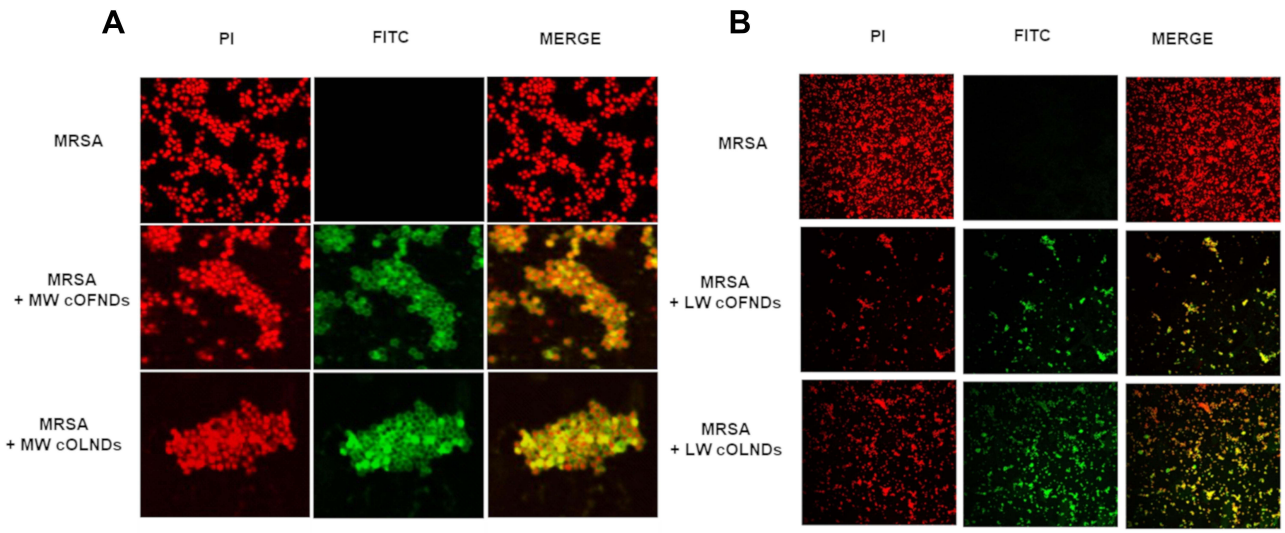

Figure 3 Confocal microscopy images of MW cND adhesion to MRSA bacterial wall and LW cND internalization by MRSA. MRSA (10^9 CFUs/mL) were left alone or incubated with 10% v/v FITC-labeled MW (**A**) or LW (**B**) cOLNDs or cOFNDs for 3 h. After staining bacteria with PI, confocal fluorescent images were taken using FITC and TRITC filters. Data are shown as representative images from three independent experiments. Red: PI. Green: FITC. Magnification: 100X.

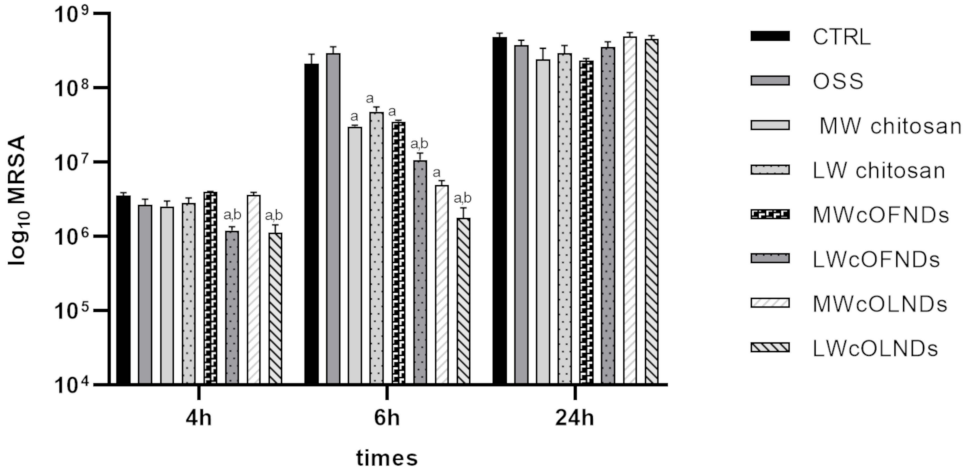

Figure 4 Anti-MRSA activity of cNDs and free chitosan. MRSA (10^4 CFUs/mL) were incubated alone or with OSS (10% v/v), free MW or LW chitosan (0.139% m/v) solution, MW or LW cOFND suspensions (10% v/v), and MW or LW cOLND suspensions (10% v/v) in sterile conditions at 37°C and their growth was monitored for 4, 6, and 24 h. At each incubation time, the samples were spread on TSA agar medium to determine the CFUs/mL. Results are shown as means ± SEM from three independent experiments and expressed as Log CFUs/mL. Data were evaluated for significance by ANOVA. Vs controls: [a] $p<0.0001$; vs MW cNDs: [b] $p<0.001$.

Confocal microscopy on the interaction between MRSA and NDs (Figure 3) showed that, starting from the earlier observational time-point (3 h) and thereafter (24 h, data not shown), MW cOLNDs and cOFNDs seemed to adhere to MRSA wall without being internalized (A), whereas LW cOLNDs and cOFNDs appeared to be avidly uptaken and internalized by the staphylococci (B). Regarding anti-staphylococcal results (Figure 4), at the earliest incubation time-point (4 h) only LW chitosan-shelled NDs significantly ($p<0.001$) reduced MRSA growth; then, after 6 h of incubation, all NDs and free chitosan solutions significantly ($p<0.001$) inhibited bacterial growth, with LW chitosan-shelled NDs being more effective than MW chitosan-shelled ones ($p<0.0001$). In the longer incubation time-point (24 h) no effects were observed for any chitosan-containing formulations.

Regarding *S. pyogenes*, as reported in Figure 5A: MW cOLND/OFNDs; B: LW cOLNDs/OFNDs, all NDs appeared to be avidly uptaken and internalized by streptococci starting from the earlier observational time-point (3 h) and up to 24 h of incubation (data not shown). Results for anti-streptococcal ND activity are shown in Figure 6: all NDs significantly

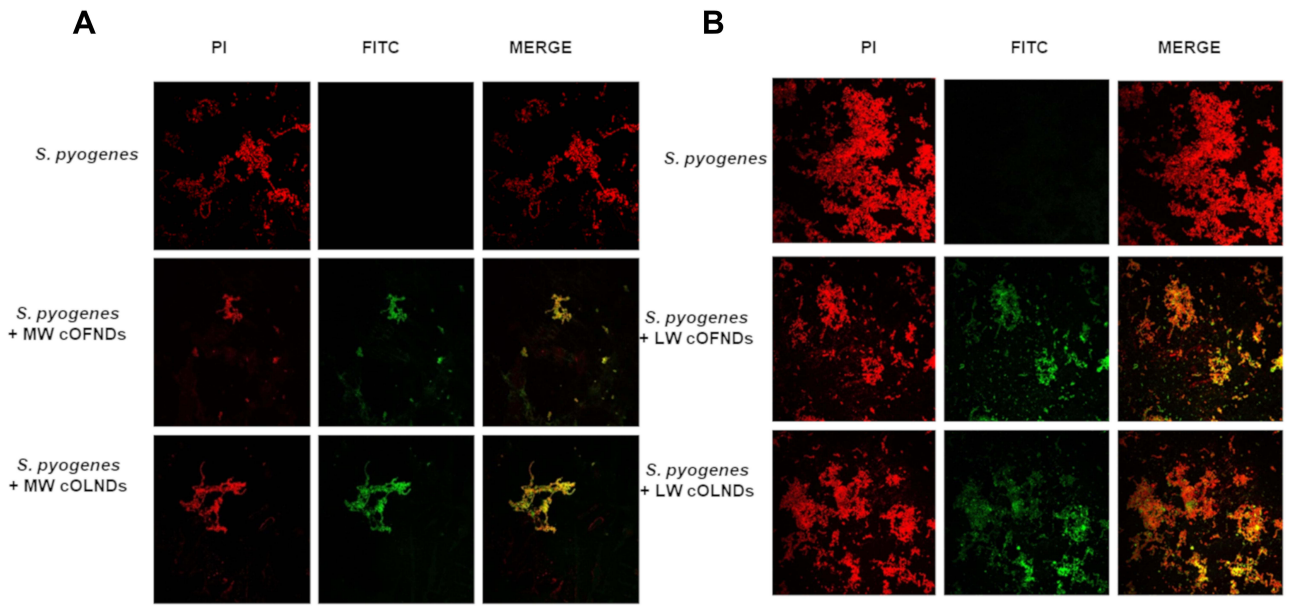

Figure 5 Confocal microscopy images of both MW and LW cND internalization by *S. pyogenes*. *S. pyogenes* (10^9 CFUs/mL) were left alone or incubated with 10% v/v FITC-labeled MW (**A**) or LW (**B**) cOFNDs or cOLNDs for 3 h. After staining bacteria with PI, confocal fluorescent images were taken using FITC and TRITC filters. Data are shown as representative images from three independent experiments. Red: PI. Green: FITC. Magnification: 100X.

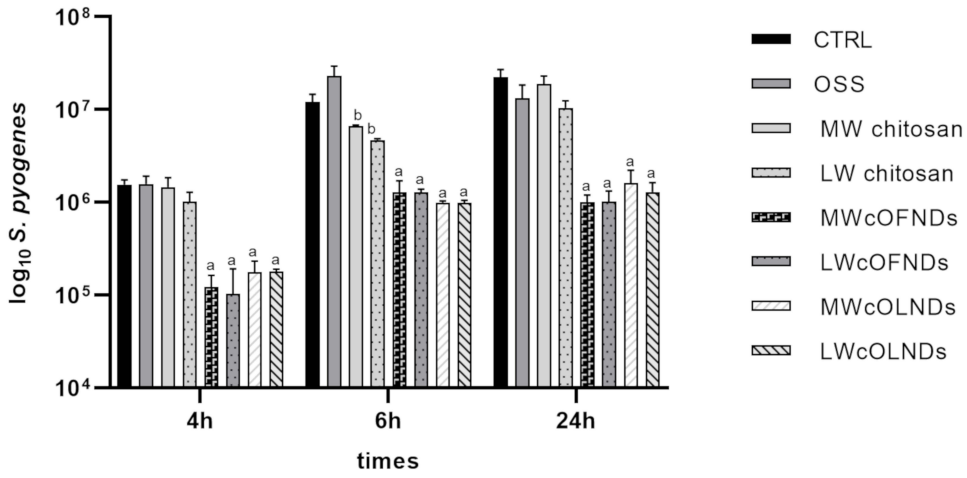

Figure 6 Anti-*S. pyogenes* activity of cNDs and free chitosan on *S. pyogenes*. *S. pyogenes* (10^4 CFUs/mL) were incubated alone or with OSS (10% v/v), free MW or LW chitosan (0.139% m/v) solution, MW or LW cOFND suspensions (10% v/v), and MW or LW cOLND suspensions (10% v/v) in sterile conditions at 37°C and their growth was monitored for 4, 6, and 24 h. At each incubation time, the samples were spread on TSA agar medium to determine the CFUs/mL. Results are shown as means ± SEM from three independent experiments and expressed as Log CFUs/mL. Data were evaluated for significance by ANOVA. vs controls: [a] $p<0.0001$; [b] $p<0.001$.

($p<0.001$) inhibited *S. pyogenes* growth up to 24 h of incubation, with no significant differences being observed between MW and LW chitosan-shelled NDs. Both MW and LW free chitosan solutions significantly ($p<0.001$) reduced bacterial growth after 6 h of incubation (Figure 6).

The physical interaction between NDs and *C. albicans* or *C. glabrata* is reported in Figure 7 and in Figure 8, respectively. In detail, all NDs appeared to be avidly uptaken and internalized by both yeasts already at the earlier observational time-point (3 h) and at the later time-point (24 h) of incubation too (data not shown). Moreover, as shown in Figure 9, all NDs and free chitosan solutions significantly ($p<0.0001$) inhibited *C. albicans* growth up to 24 h of incubation. No significant differences between MW and LW chitosan solutions and NDs were observed up to 3 h of incubation, whereas after 6 h and even more after 24 h, the inhibitory effects of LW chitosan solution and cOLNDs/

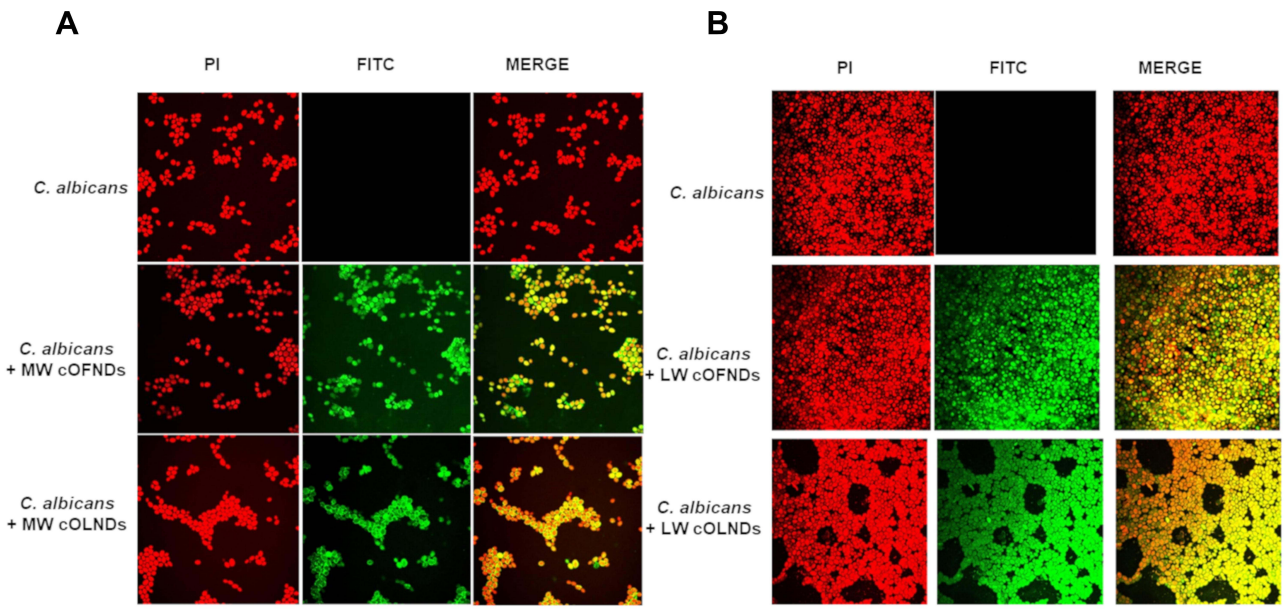

Figure 7 Confocal microscopy images of both MW and LW cND internalization by *C. albicans*. *C. albicans* (10^8 CFUs/mL) were left alone or incubated with 10% v/v FITC-labeled MW (**A**) or LW (**B**) cOFNDs or cOLNDs for 3 h. After staining yeasts with PI, confocal fluorescent images were taken using FITC and TRITC filters. Data are shown as representative images from three independent experiments. Red: PI. Green: FITC. Magnification: 100X.

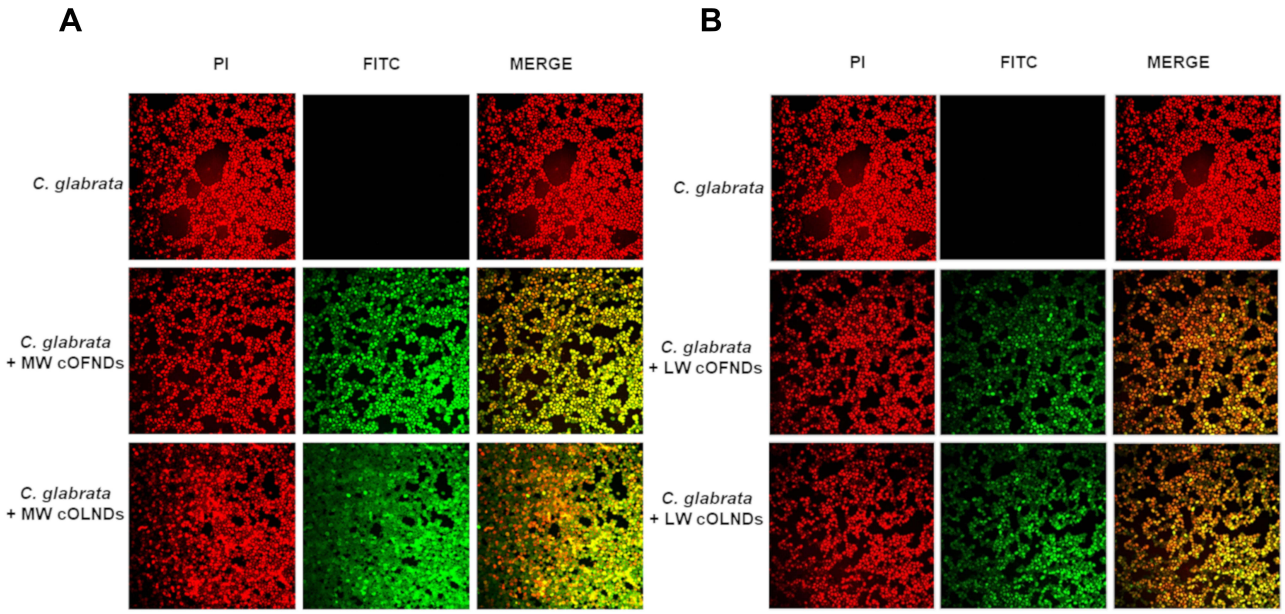

Figure 8 Confocal microscopy images of both MW and LW cND internalization by *C. glabrata*. *C. glabrata* (10^8 CFUs/mL) were left alone or incubated with 10% v/v FITC-labeled MW (**A**) or LW (**B**) cOFNDs or cOLNDs for 3 h. After staining yeasts with PI, confocal fluorescent images were taken using FITC and TRITC filters. Data are shown as representative images from three independent experiments. Red: PI. Green: FITC. Magnification: 100X.

cOFNDs on fungal growth appeared significantly ($p<0.0001$) stronger than those induced by MW chitosan solution and cOLNDs/cOFNDs. Similarly, all NDs and free chitosan solutions significantly ($p<0.0001$) inhibited *C. glabrata* growth by up to 24 h of incubation (Figure 10), but no significant differences between MW and LW chitosan solutions and NDs were observed against *C. glabrata* at any times.

Free oxygen solution did not affect either bacteria or yeast growth at any times.

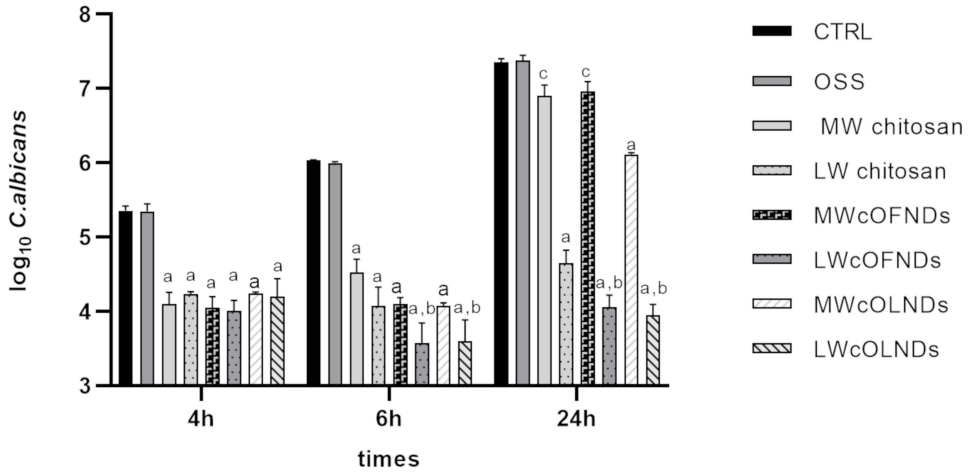

Figure 9 Anti-*C. albicans* activity of cNDs and free chitosan. *C. albicans* (10^5 CFUs/mL) were incubated alone or with OSS (10% v/v), free MW or LW chitosan (0.139% m/v) solution, MW or LW cOFND suspensions (10% v/v), and MW or LW cOLND suspensions (10% v/v) in sterile conditions at 37°C and their growth was monitored for 4, 6, and 24 h. At each incubation time, the samples were spread on SAB agar medium to determine the CFUs/mL. Results are shown as means ± SEM from three independent experiments and expressed as Log CFUs/mL. Data were evaluated for significance by ANOVA. Vs controls: [a]$p<0.0001$; vs MW cNDs: [b]$p<0.001$; Vs controls: [c]$p<0.05$.

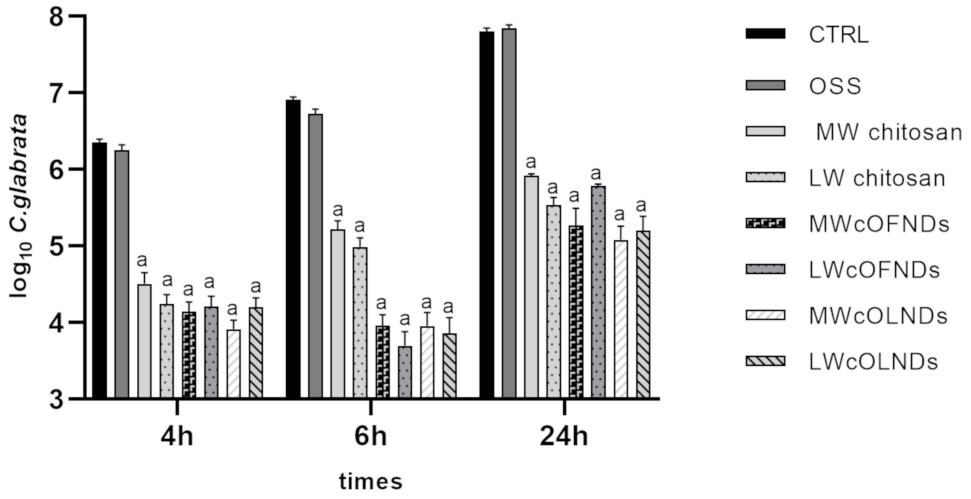

Figure 10 Anti-*C. glabrata* activity of cNDs and free chitosan. *C. glabrata* (10^5 CFUs/mL) were incubated alone or with OSS (10% v/v), free MW or LW chitosan (0.139% m/v) solution, MW or LW cOFND suspensions (10% v/v), and MW or LW cOLND suspensions (10% v/v) in sterile conditions at 37°C and their growth was monitored for 4, 6, and 24 h. At each incubation time, the samples were spread on SAB agar medium to determine the CFUs/mL. Results are shown as means ± SEM from three independent experiments and expressed as Log CFUs/mL. Data were evaluated for significance by ANOVA. Vs controls: [a]$p<0.0001$.

Discussion

The present work aimed at comparatively challenging MW and LW cOLNDs or cOFNDs for their antimicrobial properties against four CW common infectious agents: MRSA, *S. pyogenes, C. albicans*, and *C. glabrata*.

It is worth noting that chitosan, a biocompatible biopolymer, showed a wide spectrum of antimicrobial activity against Gram-positive and Gram-negative bacteria as such. Here, we investigated the activity as a component of NDs.

NDs, prepared as liquid formulations suitable for in vitro studies, are characterised by a typical core-shell structure, with DFP in the inner core and chitosan as shell component. In particular, two alternative chitosan species (MW or LW chitosan) have been considered.[29–31,39] The choice of the perfluorocarbon as the core component is crucial, as it can influence the oxygen encapsulation and effectiveness of the NDs, being able to dissolve oxygen. Since DFP carbon backbone bound ten fluorine and two hydrogen atoms, it can establish hydrogen bonds between hydrogen and oxygen

atoms. Thus, DFP is able to easily store oxygen, greatly improving its delivery into hypoxic environments.[41] Based on these premises, oxygen releasing kinetics can play a key role in the effectiveness of NDs on cell cultures.[42]

The suitability of NDs for specific applications is related to their size, composition and charge. In first-generation NDs, MW chitosan was firstly investigated as a candidate polysaccharide for the composition of the outer shell,[43] due to its biocompatibility and antimicrobial properties.[33] MW cOLNDs displayed dimensions in a nanosized range (~700 nm). On the contrary, their oxygen-free counterparts showed smaller diameters (~400 nm). Such a difference in size between oxygen-loaded and oxygen-free formulations is a direct consequence of oxygen encapsulation in NDs. A similar behaviour was previously observed for dextran-shelled oxygen loaded NDs.[24,25]

Positive charge values of about +40 mV for both NDs confirm the presence of chitosan on the ND shell surfaces and suggest the physical stability of the nanosystems. Interestingly, cationic nanocarriers are suitable for topical treatments as their positive charges interact strongly with the anionic surface of the skin. In an interesting study by Wu et al,[44] cationic fluorophore PMI-conjugated PS-NH_3^+ (amino-functionalised polystyrene latex nanoparticles) displayed brighter fluorescence at the skin surface than anionic PMI-conjugated PS-CO_2-(carboxyl-functionalised polystyrene nanoparticles).

Alongside the use of MW chitosan, here we developed LW chitosan shelled NDs taking into account the highest biocompatibility evidenced previously. Indeed, in a recent work, alternative chitosan species and derivatives were considered for shell manufacturing of second-generation NDs to improve biocompatibility with skin cells.[39] According to the results from the study, methylglycol-chitosan OLNDs were strongly reduced by 50% human keratinocyte viability and thus were excluded from the subsequent studies. Both LW and glycol chitosan-shelled OLNDs displayed cationic surfaces and ≤500 nm average diameters, with LW chitosan-shelled OLNDs being the smallest ones with the higher stability. Based on these data, LW chitosan emerged as the best candidate molecule to be compared to MW chitosan for ND manufacturing.

Notably, the biocompatibility with human cells represents a crucial issue, since the potential use in vivo of oxygen nanocarriers is related to their toxicity to eukaryotic cells. Interestingly, LW chitosan (especially chitosan with molecular weight <10,000 Da) has been reported to be associated with lower toxicity and higher water solubility compared to chitosan molecules characterised by higher molecular weight.[45] Moreover, chitosan antimicrobial activity related to nanocarriers has been reported to depend on the molecular weight and degree of deacetylation of the chitosan employed during formulation manufacturing.[46] These findings might also be exploited in the future to develop antimicrobial-loaded LW chitosan NDs as an adjuvant treatment for infected CW management.

All LW cOLNDs showed spherical shape, core-shell structure, and average diameters of ~400 nm. Such sizes are larger than those of their oxygen-free counterparts due to oxygen encapsulation, but almost half of those previously measured in first-generation MW cOLNDs.

The physico-chemical characteristics of nanocarriers are an important parameter as they can affect the nanoparticle interactions with cells. Moreover, during preclinical studies, their properties might influence the interactions with human skin and the rate and extent with which nanocarriers could be able to release the associated active molecules into the *stratum corneum*. After manufacturing and physico-chemical characterisation, MW cOLNDs and LW cOLNDs were challenged for their biocompatibility with human skin cells and for their antimicrobial properties against selected bacteria and yeasts. Indeed, the main goal was to reach the lowest cytotoxicity of human cells and the highest killing activity against pathogens. Another benefit of these NDs is the possibility to deliver oxygen to counteract hypoxia generally present in the wound environment. In our previous studies, increasing concentrations of nanocarrier suspensions were tested on human keratinocytes, with 10% v/v emerging as the most effective and less toxic concentration to be used in the subsequent experiments.[31,47]

MW and LW cOLNDs were firstly checked for biocompatibility. HaCaT cell line was chosen as a source of human keratinocytes, most represented cells (>90%) in the skin epithelium. Keratinocytes protect against pathogens, making them crucial during all wound healing stages.[2] Interestingly, the production of keratinocytic MMPs, playing crucial roles during the remodelling phase of wound healing, was demonstrated to be altered by hypoxia and dependent on the donor's age.[48] Thus, cell type and source appear to be critical in our context, since hypoxia-associated dermal pathologies are more common during the elderly.

As expected, hypoxia affected human keratinocyte viability.[31,33] MW cOLNDs did not affect the viability of human keratinocytes either in normoxia or in hypoxia, in contrast with MW cOFNDs, which were mildly toxic. On the other hand, the presence of LW chitosan in the shell of NDs (either loaded or unloaded with oxygen) led to enhanced viability of human keratinocytes (Figure 2), confirming the dependence of chitosan molecular weight on biocompatibility with HaCaT cells.[49]

NDs were also able to interact with microbial cells. As observed through confocal microscopy, MW cOLNDs were shown to physically interact with MRSA and *C. albicans*, although in a different manner (Figures 3 and 7). Indeed, NDs just adhered to MRSA cell walls, whereas they were avidly uptaken only by yeasts. Bacteria present a cell wall of peptidoglycans containing multiple glycine residues and lipoteichoic acids.[50] Although the exact molecular mechanisms have not yet been elucidated, positively charged chitosan residues (protonated amine groups) may bind to the negatively charged bacterial surface (lipoteichoic acid in Gram-positive bacteria), leading to altered membrane permeability.[51] On the other hand, *Candida* cell wall is thinner compared to that of bacteria and differs in composition due to the presence of mainly mannoproteins and β-glucans.[52] In particular, Gram-positive bacteria differ greatly from yeasts in their surface structure, and this difference can justify different interactions between nanocarriers and microbes.

These analyses were expanded to other microorganisms by using chitosan NDs only, based on their formerly mentioned advantages in terms of biocompatibility with human cells. As for *C. albicans*, MW cOLNDs were also internalised by *C. glabrata* (Figure 8). However, MW cOLNDs were also avidly uptaken by *S. pyogenes* (Figure 5), in contrast to MRSA. Notably, MRSA is characterised by a complex cell wall,[53] whereas *S. pyogenes* are covered by capsules with anti-phagocytic properties.[54] Therefore, both membranes are different in molecular composition, thus possibly justifying different interactions between chitosan nanocarriers and bacteria. However, the molecular mechanisms responsible for MW cOLND internalisation by *S. pyogenes* are yet to be elucidated. LW chitosan-shelled NDs were internalised by all four microorganisms (MRSA, *S. pyogenes, C. albicans*, and *C. glabrata*): based on these data, adhesion and internalisation were hypothesised to be associated with short-term and long-term antimicrobial effects, respectively. This hypothesis is generally confirmed by the results obtained from microbiological assays, with one exception. Indeed, whenever NDs did adhere to MRSA cell wall, their antibacterial effects lasted up to 6 hours only (Figure 4). On the contrary, all tested oxygen nanocarriers displayed long-lasting (up to 24 hours) antimicrobial effects against *S. pyogenes, C. albicans*, and *C. glabrata* upon cell internalisation (Figures 6, 9 and 10). The only exception to this pattern is represented by LW cOLND-treated MRSA: in this case, the antibacterial effects of NDs lasted for 6 hours only, despite their internalisation by bacteria. The dependence of the antimicrobial properties of NDs on the presence of chitosan in their shells appears likely, as confirmed by data obtained with the free chitosan solution alone, which are similar. Finally, the oxygen presence (OLNDs) or absence (OFNDs) within the core of all the formulations did not interfere with their antimicrobial effects against both bacteria and fungi.

The mechanisms of interaction between NDs and microorganisms can also result in leakage of intracellular constituents causing death of bacteria and yeasts. In the literature on bacteria, experimental data obtained by Helander et al provided evidence that chitosan disrupts the barrier properties of the outer membrane of Gram-negative bacteria under specific conditions.[55] Although the strongest antimicrobial activity of chitosan was observed at acidic pH, antimicrobial effects of nanocarrier at neutral pH have been reported, according to data by Jeon et al, showing that chitosan microparticles still had significant unexpected antimicrobial activity at pH 7.[56] In this context, Regiel-Futyra et al described the effects of gold chitosan-based nanocomposites on *S. aureus* and *P. aeruginosa*, observing significant and progressive damage to the cell wall.[57] The authors underlined the importance of direct contact between materials and bacteria to achieve at least bacteriostatic effects. Furthermore, they stressed that the issue of chitosan molecular weight might influence its different sites of interaction with bacterial cells. MW chitosan exerts bacteriostatic effects, which depend on the analysed bacterial strain, due to the interactions of NDs with bacterial cell wall, according to the fact that the medium molecular weight of the polymer seems to enable only surface interactions.[58]

As far as it concerns chitosan fungistatic activity, the uptake of chitosan NDs by yeasts may also cause cell wall permeabilisation resulting from binding of chitosan NDs to the surface of *Candida*. According to Peña et al, yeast permeabilisation might, in turn, cause the inhibition of main metabolic pathways, depriving cells of their energy sources.[59] Specific binding of nanocarriers to yeasts might promote K^+ efflux, extracellular acidification, inhibition of Rb^+ uptake, increased transmembrane potential difference, and increased uptake of Ca^{2+}, thus causing the inhibition of some metabolic pathways, such as respiration and fermentation.[59] These modifications regarding ion homeostasis and

metabolism may also be likely to occur with our formulations. Nevertheless, specific antifungal molecular mechanisms triggered by NDs are yet to be investigated.

Conclusion

According to the results obtained from the present study, both MW and LW cOLNDs and cOFNDs exerted long-term fungistatic activity against *C. albicans* and *C. glabrata*, long-term bacteriostatic activity against *S. pyogenes*, and short-term bacteriostatic activity against MRSA. All NDs were internalized by all bacteria and fungi, with the exception of MW cNDs, which only adhered to MRSA cell wall. On the other hand, LW cNDs displayed more advantageous physico-chemical characteristics and higher biocompatibility with human skin cells than MW cNDs. LW chitosan appeared as the best candidate for ND manufacturing: future research aimed at testing LW cND potential role for the controlled release of antimicrobial agents for reaching long-term efficacy, to treat CWs will be carried out.

Disclosure

Dr Adriano Troia reports a patent EP20140759310 in Health and Biomedical Technological area issued to Italy. The author reports no other conflicts of interest in this work.

References

1. Hong WX, Hu MS, Esquivel M, et al. The role of hypoxia-inducible factor in wound healing. *Adv Wound Care*. 2014;3(5):390–399. doi:10.1089/wound.2013.0520
2. Wang PH, Huang BS, Horng HC, Yeh CC, Chen YJ. Wound healing. *J Chin Med Assoc*. 2018;81(2):94–101. doi:10.1016/j.jcma.2017.11.002
3. Suleman L. Extracellular bacterial proteases in chronic wounds: a potential therapeutic target? *Adv Wound Care*. 2016;5(10):455–463. doi:10.1089/wound.2015.0673
4. Richard JL, Sotto A, Lavigne JP. New insights in diabetic foot infection. *World J Diabetes*. 2011;2(2):24–32. doi:10.4239/wjd.v2.i2.24
5. Sen CK, Gordillo GM, Roy S, et al. Human skin wounds: a major and snowballing threat to public health and the economy. *Wound Repair Regen*. 2009;17(6):763–771. doi:10.1111/j.1524-475X.2009.00543.x
6. Gurtner GC, Chapman MA. Regenerative medicine: charting a new course in wound healing. *Adv Wound Care*. 2016;5(7):314–328. doi:10.1089/wound.2015.0663
7. Castilla DM, Liu ZJ, Velazquez OC. Oxygen: implications for wound healing. *Adv Wound Care*. 2012;1(6):225–230. doi:10.1089/wound.2011.0319
8. Han G, Ceilley R. Chronic wound healing: a review of current management and treatments. *Adv Ther*. 2017;34(3):599–610. doi:10.1007/s12325-017-0478-y
9. Naik A, Kalia YN, Guy RH. Transdermal drug delivery: overcoming the skin's barrier function. *Pharm Sci Technol Today*. 2000;3(9):318–326. doi:10.1016/s1461-5347(00)00295-9
10. Kalliainen LK, Gordillo GM, Schlanger R, Sen CK. Topical oxygen as an adjunct to wound healing: a clinical case series. *Pathophysiology*. 2003;9(2):81–87. doi:10.1016/s0928-4680(02)00079-2
11. Ki V, Rotstein C. Bacterial skin and soft tissue infections in adults: a review of their epidemiology, pathogenesis, diagnosis, treatment and site of care. *Can J Infect Dis Med Microbiol*. 2008;19(2):173–184. doi:10.1155/2008/846453
12. Gjødsbøl K, Christensen JJ, Karlsmark T, Jørgensen B, Klein BM, Krogfelt KA. Multiple bacterial species reside in chronic wounds: a longitudinal study. *Int Wound J*. 2006;3(3):225–231. doi:10.1111/j.1742-481X.2006.00159.x
13. Saporito F, Sandri G, Bonferoni MC, et al. Essential oil-loaded lipid nanoparticles for wound healing. *Int J Nanomedicine*. 2018;13:175–186. doi:10.2147/IJN.S152529
14. Sancineto L, Piccioni M, De Marco S, et al. Diphenyl diselenide derivatives inhibit microbial biofilm formation involved in wound infection. *BMC Microbiol*. 2016;16(1):220. doi:10.1186/s12866-016-0837-x
15. Giacometti A, Cirioni O, Schimizzi AM, et al. Epidemiology and microbiology of surgical wound infections. *J Clin Microbiol*. 2000;38(2):918–922. doi:10.1128/JCM.38.2.918-922.2000
16. Shoham S, Marwaha S. Invasive fungal infections in the ICU. *J Intensive Care Med*. 2010;25(2):78–92. doi:10.1177/0885066609355262
17. Ballard J, Edelman L, Saffle J, et al. Positive fungal cultures in burn patients: a multicenter review. *J Burn Care Res*. 2008;29(1):213–221. doi:10.1097/BCR.0b013e31815f6ecb
18. Mlinaric Missoni E, Vukelic M, de Soy D, Belicza M, Vazic Babic V, Missoni E. Fungal infection in diabetic foot ulcers. *Diabet Med*. 2005;22(8):1124–1125. doi:10.1111/j.1464-5491.2005.01611.x
19. Kim J, Sudbery P. Candida albicans, a major human fungal pathogen. *J Microbiol*. 2011;49(2):171–177. doi:10.1007/s12275-011-1064-7
20. Papon N, Courdavault V, Clastre M, Bennett RJ. Emerging and emerged pathogenic Candida species: beyond the Candida albicans paradigm. *PLoS Pathog*. 2013;9(9):e1003550. doi:10.1371/journal.ppat.1003550
21. Turner SA, Butler G. The Candida pathogenic species complex. *Cold Spring Harb Perspect Med*. 2014;4(9):a019778. doi:10.1101/cshperspect.a019778
22. Confederat LG, Tuchilus CG, Dragan M, Sha'at M, Dragostin OM. Preparation and antimicrobial activity of Chitosan and its derivatives: a concise review. *Molecules*. 2021;26(12):3694. doi:10.3390/molecules26123694
23. Abd El-Hack ME, El-Saadony MT, Shafi ME, et al. Antimicrobial and antioxidant properties of chitosan and its derivatives and their applications: a review. *Int J Biol Macromol*. 2020;164:2726–2744. doi:10.1016/j.ijbiomac.2020.08.153

24. Rozman NAS, Tong WY, Leong CR, Tan WN, Hasanolbasori MA, Abdullah SZ. Potential antimicrobial applications of Chitosan Nanoparticles (ChNP). *J Microbiol Biotechnol*. 2019;29(7):1009–1013. doi:10.4014/jmb.1904.04065
25. Rocha Neto JBM, Lima GG, Fiamingo A, et al. Controlling antimicrobial activity and drug loading capacity of chitosan-based layer-by-layer films. *Int J Biol Macromol*. 2021;172:154–161. doi:10.1016/j.ijbiomac.2020.12.218
26. Liu Y, Xiao Y, Cao Y, Guo Z, Li F, Wang L. Construction of Chitosan-based hydrogel incorporated with antimonene nanosheets for rapid capture and elimination of bacteria. *Adv Funct Mater*. 2020;30(35):2003196. doi:10.1002/adfm.202003196
27. Han D, Li Y, Liu X, et al. Rapid bacteria trapping and killing of metal-organic frameworks strengthened photo-responsive hydrogel for rapid tissue repair of bacterial infected wounds. *Chem Eng J*. 2020;396:125194. doi:10.1016/j.cej.2020.125194
28. Feng Z, Liu X, Tan L, et al. Electrophoretic deposited stable Chitosan@MoS2 coating with rapid in situ bacteria-killing ability under dual-light irradiation. *Small*. 2018;14(21):1704347. doi:10.1002/smll.201704347
29. Cavalli R, Bisazza A, Rolfo A, et al. Ultrasound-mediated oxygen delivery from chitosan nanobubbles. *Int J Pharm*. 2009;378(1–2):215–217. doi:10.1016/j.ijpharm.2009.05.058
30. Cavalli R, Bisazza A, Giustetto P, et al. Preparation and characterization of dextran nanobubbles for oxygen delivery. *Int J Pharm*. 2009;381(2):160–165. doi:10.1016/j.ijpharm.2009.07.010
31. Magnetto C, Prato M, Khadjavi A, et al. Ultrasound-activated decafluoropentane-cored and chitosan-shelled nanodroplets for oxygen delivery to hypoxic cutaneous tissues. *RSC Adv*. 2014;4(72):38433–38441. doi:10.1039/C4RA03524K
32. Prato M, Magnetto C, Jose J, et al. 2H,3H-decafluoropentane-based nanodroplets: new perspectives for oxygen delivery to hypoxic cutaneous tissues. *PLoS One*. 2015;10(3):e0119769. doi:10.1371/journal.pone.0119769
33. Banche G, Prato M, Magnetto C, et al. Antimicrobial chitosan nanodroplets: new insights for ultrasound-mediated adjuvant treatment of skin infection. *Future Microbiol*. 2015;10(6):929–939. doi:10.2217/fmb.15.27
34. Riess JG, Krafft MP. Fluorinated materials for in vivo oxygen transport (blood substitutes), diagnosis and drug delivery. *Biomaterials*. 1998;19(16):1529–1539. doi:10.1016/s0142-9612(98)00071-4
35. Mazzaccaro D, Ticozzi R, D'Alessandro S, et al. Effect of antibiotic-loaded chitosan nanodroplets on Enterococci isolated from chronic ulcers of the lower limbs. *Future Microbiol*. 2020;15:1227–1236. doi:10.2217/fmb-2019-0255
36. Gulino GR, Magnetto C, Khadjavi A, et al. Oxygen-loaded nanodroplets effectively abrogate hypoxia dysregulating effects on secretion of MMP-9 and TIMP-1 by human monocytes. *Mediators Inflamm*. 2015;2015:964838. doi:10.1155/2015/964838
37. Prato M, Khadjavi A, Magnetto C, et al. Effects of oxygen tension and dextran-shelled/2H,3H-decafluoropentane-cored oxygen-loaded nanodroplets on secretion of gelatinases and their inhibitors in term human placenta. *Biosci Biotechnol Biochem*. 2016;80(3):466–472. doi:10.1080/09168451.2015.1095068
38. Khadjavi A, Stura I, Prato M, et al. "In Vitro", "In Vivo" and "In Silico" Investigation of the anticancer effectiveness of oxygen-loaded Chitosan-shelled nanodroplets as potential drug vector. *Pharm Res*. 2018;35(4):75. doi:10.1007/s11095-018-2371-z
39. Argenziano M, Bressan B, Luganini A, et al. Comparative evaluation of different Chitosan species and derivatives as candidate biomaterials for oxygen-loaded nanodroplet formulations to treat chronic wounds. *Mar Drugs*. 2021;19(2):112. doi:10.3390/md19020112
40. Sze A, Erickson D, Ren L, Li D. Zeta-potential measurement using the Smoluchowski equation and the slope of the current-time relationship in electroosmotic flow. *J Colloid Interface Sci*. 2003;261(2):402–410. doi:10.1016/S0021-9797(03)00142-5
41. Tsai WT. Environmental hazards and health risk of common liquid perfluoro-n-alkanes, potent greenhouse gases. *Environ Int*. 2009;35(2):418–424. doi:10.1016/j.envint.2008.08.009
42. Dietz I, Jerchel S, Szaszák M, Shima K, Rupp J. When oxygen runs short: the microenvironment drives host-pathogen interactions. *Microbes Infect*. 2012;14(4):311–316. doi:10.1016/j.micinf.2011.11.003
43. Dougherty TJ, Pucci MJ. *Antibiotic Discovery and Development*. Springer Science & Business Media; 2014:1127. doi:10.1007/978-1-4614-1400-1
44. Wu X, Landfester K, Musyanovych A, Guy RH. Disposition of charged nanoparticles after their topical application to the skin. *Skin Pharmacol Physiol*. 2010;23(3):117–123. doi:10.1159/000270381
45. Park JH, Saravanakumar G, Kim K, Kwon IC. Targeted delivery of low molecular drugs using chitosan and its derivatives. *Adv Drug Deliv Rev*. 2010;62(1):28–41. doi:10.1016/j.addr.2009.10.003
46. Seyfarth F, Schliemann S, Elsner P, Hipler UC. Antifungal effect of high- and low-molecular-weight chitosan hydrochloride, carboxymethyl chitosan, chitosan oligosaccharide and N-acetyl-D-glucosamine against Candida albicans, Candida krusei and Candida glabrata. *Int J Pharm*. 2008;353(1–2):139–148. doi:10.1016/j.ijpharm.2007.11.029
47. Khadjavi A, Magnetto C, Panariti A, et al. Chitosan-shelled oxygen-loaded nanodroplets abrogate hypoxia dysregulation of human keratinocyte gelatinases and inhibitors: new insights for chronic wound healing. *Toxicol Appl Pharmacol*. 2015;286(3):198–206. doi:10.1016/j.taap.2015.04.015
48. Xia YP, Zhao Y, Tyrone JW, Chen A, Mustoe TA. Differential activation of migration by hypoxia in keratinocytes isolated from donors of increasing age: implication for chronic wounds in the elderly. *J Invest Dermatol*. 2001;116(1):50–56. doi:10.1046/j.1523-1747.2001.00209.x
49. Wiegand C, Winter D, Hipler UC. Molecular-weight-dependent toxic effects of chitosans on the human keratinocyte cell line HaCaT. *Skin Pharmacol Physiol*. 2010;23(3):164–170. doi:10.1159/000276996
50. Navarre WW, Schneewind O. Surface proteins of gram-positive bacteria and mechanisms of their targeting to the cell wall envelope. *Microbiol Mol Biol Rev*. 1999;63(1):174–229. doi:10.1128/MMBR.63.1.174-229.1999
51. Liu H, Du Y, Wang X, Sun L. Chitosan kills bacteria through cell membrane damage. *Int J Food Microbiol*. 2004;95(2):147–155. doi:10.1016/j.ijfoodmicro.2004.01.022
52. Chaffin WL, López-Ribot JL, Casanova M, Gozalbo D, Martínez JP. Cell wall and secreted proteins of Candida albicans: identification, function, and expression. *Microbiol Mol Biol Rev*. 1998;62(1):130–180. doi:10.1128/MMBR.62.1.130-180.1998
53. Brown S, Santa Maria JP, Walker S. Wall teichoic acids of gram-positive bacteria. *Annu Rev Microbiol*. 2013;67(1):313–336. doi:10.1146/annurev-micro-092412-155620
54. Patterson MJ. Streptococcus. In: Baron S, editor. *Medical Microbiology*. 4th ed. University of Texas Medical Branch at Galveston: 1996. Available from: http://www.ncbi.nlm.nih.gov/books/NBK7611/.
55. Helander IM, Nurmiaho-Lassila EL, Ahvenainen R, Rhoades J, Roller S. Chitosan disrupts the barrier properties of the outer membrane of gram-negative bacteria. *Int J Food Microbiol*. 2001;71(2–3):235–244. doi:10.1016/s0168-1605(01)00609-2

56. Jeon SJ, Oh M, Yeo WS, Galvão KN, Jeong KC. Underlying mechanism of antimicrobial activity of chitosan microparticles and implications for the treatment of infectious diseases. *PLoS One*. 2014;9(3):e92723. doi:10.1371/journal.pone.0092723
57. Regiel-Futyra A, Kus-Liśkiewicz M, Sebastian V, et al. Development of noncytotoxic chitosan-gold nanocomposites as efficient antibacterial materials. *ACS Appl Mater Interfaces*. 2015;7(2):1087–1099. doi:10.1021/am508094e
58. Rai A, Prabhune A, Perry C. Antibiotic mediated synthesis of gold nanoparticles with potent antimicrobial activity and their application in antimicrobial coatings. *J Mater Chem*. 2010:20. doi:10.1039/c0jm00817f
59. Peña A, Sánchez NS, Calahorra M. Effects of chitosan on Candida albicans: conditions for its antifungal activity. *Biomed Res Int*. 2013;2013:527549. doi:10.1155/2013/527549